AD A026293

THE RESPONSE OF COATED STEELS TO CAVITATION IN CORROSIVE ENVIRONMENTS

C. M. Preece, H. Herman, V. Wilms, S. Safai, J. Fauty
Department of Materials Science
The State University of New York at Stony Brook
Stony Brook, N. Y. 11794

May 1976

TR-1

Technical Report No. 1

to

The Office of Naval Research

Contract No. N00014-75-C-1018 NR036-110

NR-036-110

DDC
RECEIVED
JUN 30 1976
A

DISTRIBUTION STATEMENT A
Approved for public release;
Distribution Unlimited

Reproduction in whole or in part is permitted for any purpose of the United States Government.

I. INTRODUCTION

Protective coatings have been applied to metals and alloys by thermal spraying techniques for many decades to provide resistance to corrosion. Although the coatings always contain some porosity and, therefore, would not be expected to provide complete protection, they have proven remarkably successful. For example, aluminum coated steels, with and without a polymer top coat, have been subjected to salt water and industrial corrosion tests of 12 and 19 years duration, respectively[1,2], and are found to exhibit exceptionally little evidence of corrosive attack. It has been postulated[3] that the initial products of corrosion might fill the pores and, thereby, block any further corrosion. However, the origin and nature of the pores and the mechanism of corrosion inhibition have not been thoroughly investigated from an electrochemical viewpoint. Moreover, in marine environments, structures are frequently subjected to mechanical erosion by sand particles, cavitation or liquid impact, and the combined effects of erosion and corrosion have received very little attention.

The investigation under this contract was initiated in June 1975 to provide some understanding of the mechanism(s) of deterioration of plasma sprayed coatings by erosion and/or corrosion. It is apparent that such an understanding will require an extensive long range investigation covering a wide range of coatings and of erosive and corrosive environments. However, in order to allow the problem areas to be defined, attention has been focussed on a single ceramic coating, alumina, and a single metallic coating, aluminum, both on steel substrates. In the initial phase of this program, emphasis has been on the structural and mechanical characterization of the coating itself with some preliminary studies of their response to cavitation.

II. PLASMA SPRAYED COATINGS

The plasma guns used in this program are non-transferred d.c. arc devices with a powder feeder illustrated schematically in Fig. 1. The working gas (usually argon, nitrogen, helium, hydrogen or mixtures of these gases) enters the plasma region, at which point an arc is initially struck (in our equipment, by a high frequency electrical pulse) between the cathode and the water-cooled anode. A high temperature plasma of ions, molecules and electrons is thus formed. This plasma can be maintained by the correct geometrical configuration, thermal balance and flow of new gas. The plasma exists from the front nozzle with temperatures between 5,000° and 10,000°K and at velocities near sonic. The powdered coating material, is fed into the plasma at the nozzle, is melted and impelled towards the substrate.

Such a system has the following advantages over alternative coating processes: (i) the temperatures are sufficiently high to melt any material; (ii) the exit velocities are so great that, under controlled conditions, solidification of the fused material does not occur before it strikes the substrate; (iii) inert gases can be used for the plasma which minimize contamination of the coating or, alternatively, the use of reducing gases can eliminate oxidation and (iv) by varying the powder composition, graded coatings, designed to minimize mismatching of mechanical and chemical properties between coating and substrate can be produced.

For studies of the coating/substrate system, coupons of 1018 steel were cleaned and grit blasted prior to the spraying with aluminum or alumina, in order to provide a roughened surface for mechanical interlocking of the coating. In addition, samples of aluminum, alumina and Al_2O_3-Y_2O_3 mixtures have been sprayed and removed from the substrate to allow a study to be made of their porosity, macro-, micro- and crystal-structures. Removal of the coating was

achieved by spraying the substrate with a concentrated NaCl solution prior to applying the coating. This treatment deposited a thin layer of NaCl (<1 μm) which was subsequently dissolved allowing the coating to be removed intact.

III. CHARACTERIZATION OF ALUMINUM COATINGS

(i) Microstructure

During the process of plasma spraying, the individual powder particles are superheated in the plasma gun to temperatures well above their melting temperature and impinge on the substrate at velocities which may approach that of sound. Since the substrate is highly conducting, solidification is very rapid: the cooling rates have been determined for plasma sprayed metals by measurement of the dimensions of the microstructural features and are reported to be in the range of 10^6 - 10^8°C/sec.[4]. Thus, the coating can be considered as being effectively splat quenched from the liquid state. The resulting microstructure consists of flattened platelets of the metal with pores of varying size between the particles, Fig. 2. The grain size within the particles was too fine to be resolved by optical or scanning electron microscopy (SEM), but was revealed by over-etching a thin foil sample for transmission electron microscopy (TEM), Fig. 3. This micrograph is of a section parallel to the substrate and shows the extremely fine scale of the grains, 0.05 - 0.10 μm in dia.

To avoid the etching problem associated with the electrochemical thinning of samples and to enable a section perpendicular to the substrate to be examined, an ion-thinning technique was employed. While this technique reveals the columnar form of the grains, Fig. 4, it has the disadvantage of heating the sample. Evidence that recovery has taken place is given by subgrain arrays of dislocations observed in several grains. The annealing may account for the larger grain size observed in the ion-thinned samples compared with those in the electrochemically prepared samples.

(ii) Porosity

The size, total volume and distribution of pores in a sprayed coating influence both its strength and permeability and, hence, play a major role in determining its protective qualities. It was deemed essential, therefore, to characterize the pore content of the coatings sprayed in this investigation. The technique used for aluminum coatings was mercury porosimetry in combination with stereo-microscopy.

Mercury intrusion porosimetry is a convenient tool and has been applied extensively to the study of cements and other porous materials[5-7]. It has the advantage of covering a large range of pore sizes but is limited to the measurement of those pores which are connected to the surface. There are also errors in the measurements due to "bottle-neck" pores, compressability of the mercury and the sample, wetting and/or interaction between the mercury and the sample, etc. In the case of aluminum, wetting and interaction are only important (i) if the aluminum oxide is removed and (ii) in the presence of moist air or water. Since neither of these conditions was in effect during the measurements, these factors were not considered to influence the results significantly.

Many spraying parameters play a role in determining the pore content of coatings. However, it was decided that the study should concentrate, at least initially, on those two parameters which have the greatest effect and are easiest to control, namely gun to work piece distance[8, 9] and coating thickness.

Fig. 5 shows the variation of penetration volume versus pressure (which is proportional to pore size*) for three different spraying distances, ℓ.

---

*The applied pressure, P, necessary to fill a pore of diameter, d, is given by[10]:

$$P = -\frac{4\gamma \cos\theta}{d}$$

where γ and θ are the surface tension of the mercury and contact angle between mercury and solid, respectively.

The total pore volumes are given in Fig. 6. In theory, the porosity should increase continuously with increasing values of ℓ, whereas the present results show a minimum value at the intermediate distance. The higher porosity value at the lowest spraying distance is attributed to severe superheating of the aluminum. This results in some atomization of the metal and the entrapment of gases during spraying and produces a sponge-like structure with a large density of small pores. This structure is illustrated in Fig. 7. Similar behavior has been observed in Al_2O_3[11].

The influence of coating thickness on porosity was examined over a range of thicknesses of 0.45 - 1.2 mm. Fig. 8 shows that, for any cumulative pore volume, the pore size distribution shifts towards larger pore diameters as the thickness of the coating is decreased. The total pore volume also increases with decreasing thickness, Fig. 9. However, because the surface to volume ratio decreases as the thickness increases, this apparent decrease in porosity may be attributed in part to the greater ratio of closed internal pores to those connected to the surface.

III. CHARACTERIZATION OF ALUMINA COATINGS

(i) Crystallography

X-ray Debye-Scherrer, diffractometry techniques and electron diffraction have been used to determine the structure and composition of the phases in plasma sprayed alumina. In the case of pure alumina, a number of metastable, high temperature phases are observed instead of the equilibrium α (corundum) structure. These findings have been reported earlier by other researchers[12-14]. However, in the present investigation, a relationship has been observed between the specific polymorphs of alumina present and the spray process parameters. In plasma sprayed coatings of thickness < 250 μm, the common high temperature phases are δ and θ with some γ and α, whereas in the samples produced

by the lower temperature, oxyacetylene spray process, the common phase is γ with some Θ and α. In thick plasma sprayed coatings (> 250 μm) also, the main phases are γ and α with very little δ and Θ being observed. The implication of this result is that thicker coatings have a slower cooling rate due both to the poor conductivity of a ceramic and to the reheating of the material already deposited by the repeated traversing of the plasma gun. This allows the structure to equilibrate to the stable corundum phase.

(ii) Microstructure

The microstructure of these ceramic coatings, observed by SEM and shown in Fig. 10 is similar to that of the aluminum in that it consists of flattened platelets which contain fine columnar grains. The latter, however, are larger than those in the metal, being ~3 μm long and ~1 μm in dia. This is probably due to the slower cooling rates in the ceramics (10^4 - 10^6 °C/sec.). In addition, numerous cracks and fissures, both interparticle and transparticle (the latter being intergranular) are observed. These are attributed to thermal shock and the difference in thermal contraction between coating and substrate.

The microstructure and phase-identification were further investigated by TEM. Samples were prepared from the plasma sprayed material by low angle ion-thinning as shown in Fig. 11. Electron diffraction confirmed the existance of metastable polymorphs and also that the initially sprayed layers of the coating are amorphous. The latter are due to the extremely rapid quench rate of the initial layers. The cooling rate decreases as the coating is built up, as described earlier, and subsequent layers are, therefore, crystalline.

The grains of the crystalline regions were found to be essentially defect free in contrast to the observations of hexagonal dislocation networks in conventionally prepared alumina. However, such defect-free, fine grained

structures have been reported in splat quenched specimens[15,16].

(iii) The Alumina/Steel Bond

An electron microprobe study has been made of the degree of chemical interaction between the oxide and the steel substrate. The results for samples in the as-sprayed condition and after a subsequent annealing treatment are illustrated in Fig. 12. It is apparent that there is significant incorporation of iron into the alumina with considerably less diffusion of aluminum into the substrate. Moreover, the annealing treatments of 2 and 6 hrs. in argon at 1,100°C have little influence on the interactions at the interface. It appears probable, therefore, that the oxides on the iron, produced before or during the first passage of the plasma torch, are dissolved by the molten alumina. This has been shown to occur in other studies of ceramic/metal interactions, in which the presence of an oxide on the metal was found to be essential to the formation of a satisfactory bond[17,18].

The adhesion of the coating to the substrate is usually determined by a standard test (ASTM designation: C633-69 or DIN 50160), in which a coating of > 375 μm is sprayed onto a 2.54 cm dia. mandrel. Subsequently, the coated mandrel and a second, as-machined mandrel are adhered together with an epoxy resin. After normal curing, they are tested in tension. If, on failure, the coating has completely parted from its substrate, the test is considered to be valid. The results of tests using the above technique are given in Fig. 13.

A major objection to this test, however, is the need to employ epoxy resin, since the resin permeates the porous coating and the results obtained may, in fact, be for a coating-resin composite. A new adhesion test has, therefore, been devised which does not employ resin. Thus, the value of adhesion strength obtained is actually that of bond strength (of the coating itself or of the interface, whichever fails). In this test, a flat-topped

cone is inserted into a matched socket and the two surfaces are machined flat. The coating is then applied to this prepared surface and the two sections are pulled apart. The principal advantage of this test is that the coating is not modified in any way and the surface is not affected. It is, therefore, singularly appropriate for testing coatings which have been exposed to corrosive and/or cavitating environments.

(iv) Mixed Alumina-Yttria Coatings

Additions of small amounts of yttrium to commercial superalloys have been found to significantly increase their corrosion resistance: it is thought that the yttrium improves the adhesion of the naturally formed oxide on these alloys, thereby reducing the probability of spalling during thermal cycling. It was postulated, therefore, that yttrium might have similar beneficial effects on the adhesion of sprayed oxide coatings. Consequently, "alloy" powders of Al_2O_3 with 3-20% Y_2O_3 were prepared by mechanically mixing the constituents together and sintering and ball milling the product. The powders were then sprayed onto steel substrates.

Additions of yttria to alumina do have a significant effect on the structure and properties of the coating. These mixed oxides have a two phase structure consisting of crystalline Al_2O_3 (presumably containing some yttrium) in an amorphous, yttrium rich matrix. The porosity of the oxides, determined by small angle neutron scattering*, was found to decrease with increasing yttria content. Moreover, the yttria produced an increase in

---

* This study was made at Kernforschungsanlage, Julich, Germany as part of a joint NATO program between H. Herman and W. Schmatz

the adhesive strength of the coating/substrate interface as indicated in Fig. 13. The beneficial effects of the yttria are attributed to the amorphous second phase which becomes rigid at a temperature well below the solidification temperature of Al_2O_3 (2060°C). It is, therefore, able to flow more readily and (a) interact with the grit blasted substrate surface and (b) fill the interstices between the platelets of crystalline oxide, thereby increasing the adhesion and reducing the porosity, respectively.

IV. CAVITATION EROSION OF ALUMINA COATINGS

Plasma sprayed alumina coatings were subjected to cavitation produced in distilled water by a vibratory probe operating at 30KHz and an amplitude of ~20 μm. The erosion behavior of the coatings sprayed in three different torch gas atmospheres, namely pure argon, Ar + 5% H_2 and Ar + 6.5% H_2, is characterized by the plots of weight loss versus time of exposure to cavitation in Fig. 14. A feature common to all three plots is the absence of an incubation period which is normally observed in cavitation experiments. The maximum rate of weight loss occurs in the early stages of attack (in the first 10 minutes) after which it gradually decreases to a steady state value.

The data indicate that the erosion resistance of plasma sprayed alumina increases significantly with increasing hydrogen content of the torch gas. This may be attributed to the fact that the hydrogen raises the temperature of the plasma. Thus, the Al_2O_3 particles would be superheated to a higher temperature and, on impacting the substrate surface, remain molten longer and, therefore, have more time to flow and develop both mechanical and chemical bonds.

Further evidence that slower cooling rates increase the cohesion between particles is given by measurements on samples of different thickness. An 0.84 mm coating was found to be considerably more resistant to cavitation

than a sample of 0.30 mm thickness. The former exhibited an initial, small weight loss in the first 5 minutes of exposure (which was attributed to the erosion of loosely bonded particles) after which there was no detectable weight loss during the next 10 minute exposure. The thinner coating, on the other hand, did not exhibit any incubation period and had a much more rapid rate of weight loss.

Since adhesion tests indicate that the coating/substrate adhesion is weaker than the interparticle bonding, erosion of the coatings had been expected to occur by spalling at the interface. However, this was not the case. Material loss, resulting from exposure of the alumina coating to cavitation, was by particle removal and was somewhat random in nature - the weakest areas of the coating being attacked more severely than the rest - as shown in Fig. 15. These preferential erosion pits can be more detrimental than general particle removal since areas of the substrate at the bottom of the pits can become exposed to erosion and corrosion attack much sooner.

The progressive development of surface damage in Al_2O_3 by cavitation is shown in Fig. 16. Between 0 and 2 minutes exposure, Figs. 16a-c, the incipient cracks begin to widen and separate allowing the more loosely held particles to be eroded away. After 2 minutes exposure, the fracture surface becomes visible, Fig. 16c and, after 3-4 minutes almost all the particles in the vicinity of the damage zones have separated from one another and major material removal has occurred. The pores initially present in the as-sprayed coating do not appear to play a significant role in the erosion process.

V. REFERENCES

1. American Welding Society Corrosion Tests of Metallized Coated Steels, 12 Year Report, AWS Report #C2.11-67 (1967).

2. "Corrosion Tests of Flame Sprayed Coated Steels", American Welding Society 19 Year Report, AWS Report #C2.14-74 (1974).

3. R. E. Mansford, Corrosion Technology Corr, Tech. 3 314 (1956).

4. M. Moss, D. L. Smith and R. A. Lefever, Appl. Phys. Let. 5 120 (1964).

5. D. N. Winslow and S. Diamond, J. Mat. Sci. 5 564 (1970).

6. S. Diamond, Cement and Concrete Research 1 531 (1971).

7. A. Auskern and W. Horn, J. of Testing and Evaluation (ASTM) 1 74 (1973).

8. D. M. Karpinos, Soviet Powder Metallurgy and Metal Ceramics No. 8 (140) 41 (1974).

9. L. O. Svirskii and Yu. A. Pirogev, "Heat Resistant Coatings" p. 135, Ed. M. A. Toropov, Consultants Bureau, N. Y. (1967).

10. E. W. Washburn, Phys. Rev. 17 273 (1921).

11. F. J. Kaubeck, Proc. 3rd Annual Scanning Electron Microscopy Symposium, IITRI (1970).

12. H. Meyer, Werkstoff and Korrosion 11 601 (1960).

13. N. N. Ault, J. Am. Ceramic Soc. 40 69 (1957).

14. F. Eichhorn and J. Metzler, Metalloberfläche 26 212 (1972).

15. R. Stoering and H. Conrad, Acta Met. 17 933 (1969).

16. S. Agarwal and H. Herman, Siemen's Review 41 (7th Special Issue) 34 (1974).

17. J. W. McLean, "Scientific Aspects of Dental Materials", p. 307, ed. J. A. von Fraunhofer, Butterworth Press, London (1975).

18. C. Helgesson, "Ceramic to Metal Bonding", (1960).

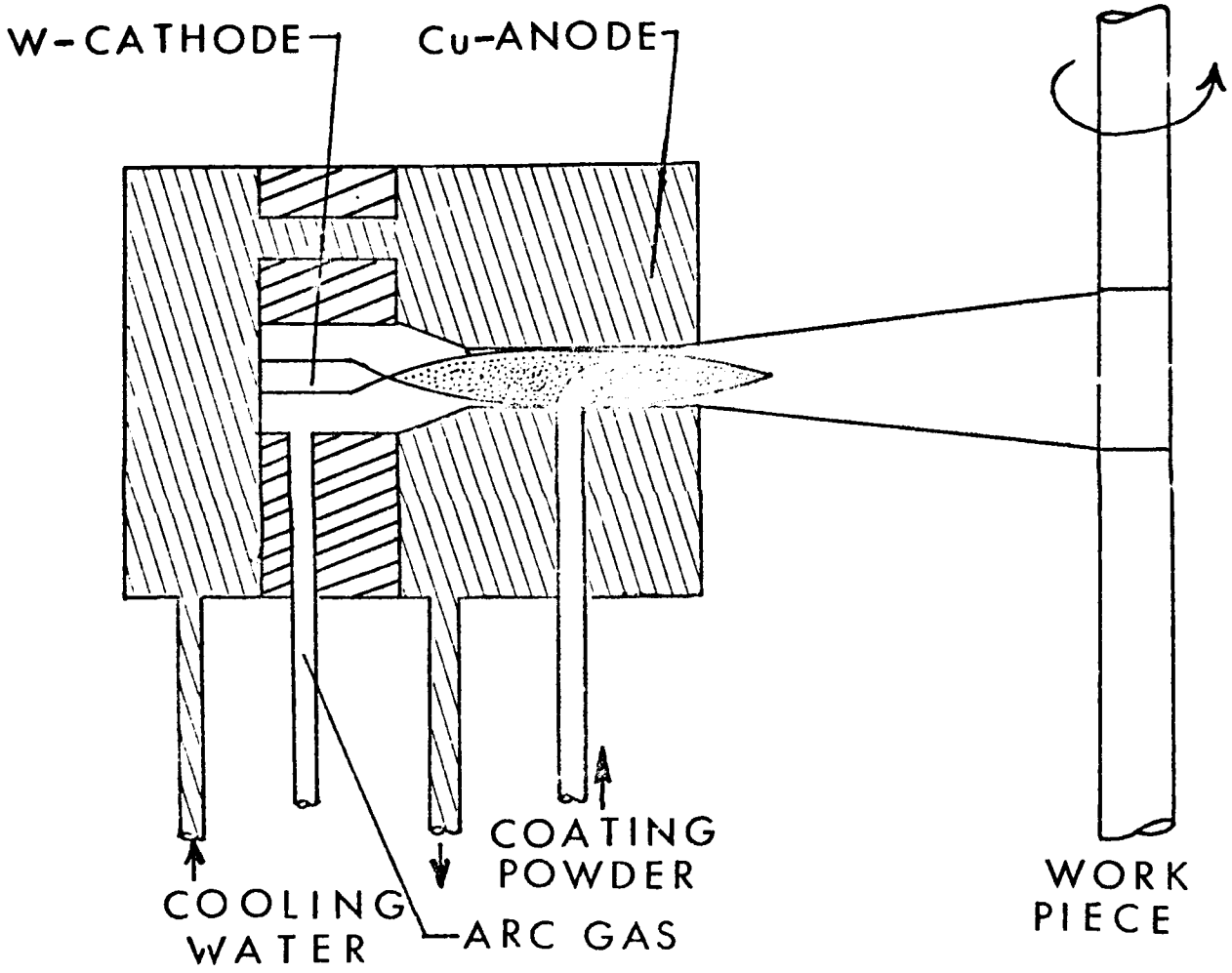

Fig. 1 The Plasma Gun (schematic).

Fig. 2. Scanning electron micrograph of polished surface of 0.6 mm thick aluminum coating.

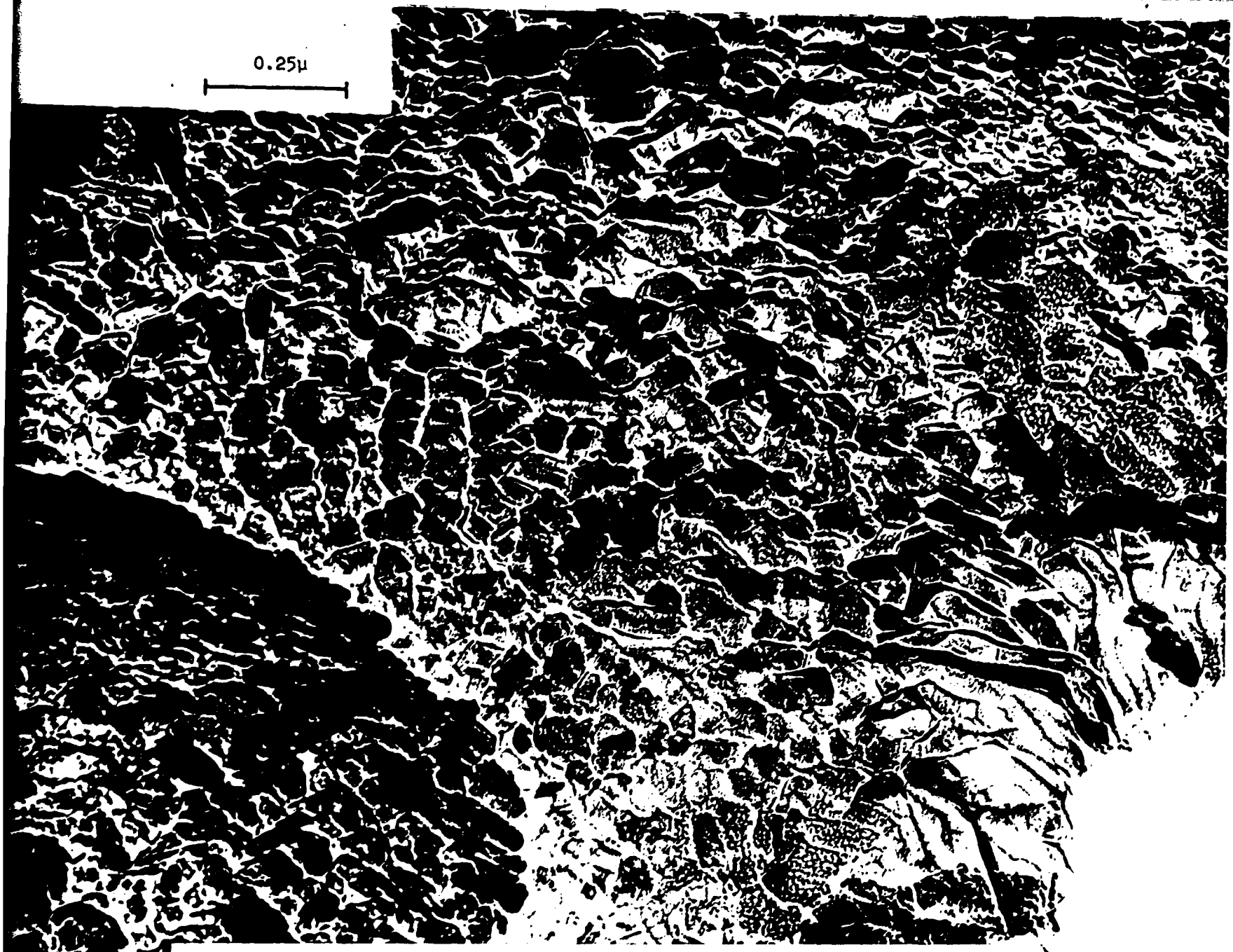

Fig. 3. Transmission electron micrograph of a section of aluminum parallel to the substrate, showing ultra-fine grain structures.

Fig. 4. Transmission electron micrograph of a section of aluminum perpendicular to the substrate showing columnar grain structure.

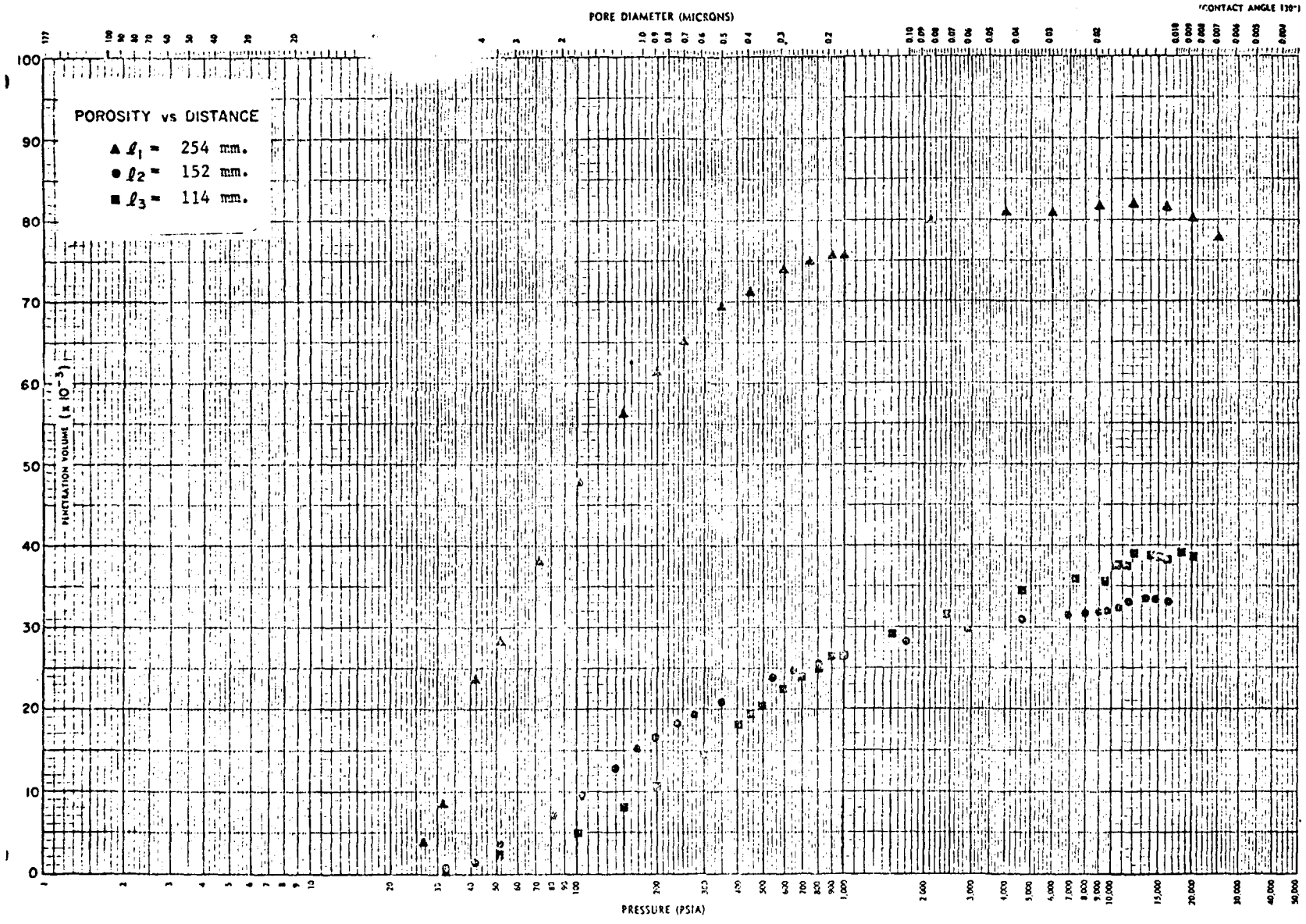

Fig. 5. Penetration of mercury into the coating versus applied pressure for aluminum coatings sprayed at different distances, ℓ, from the gun.

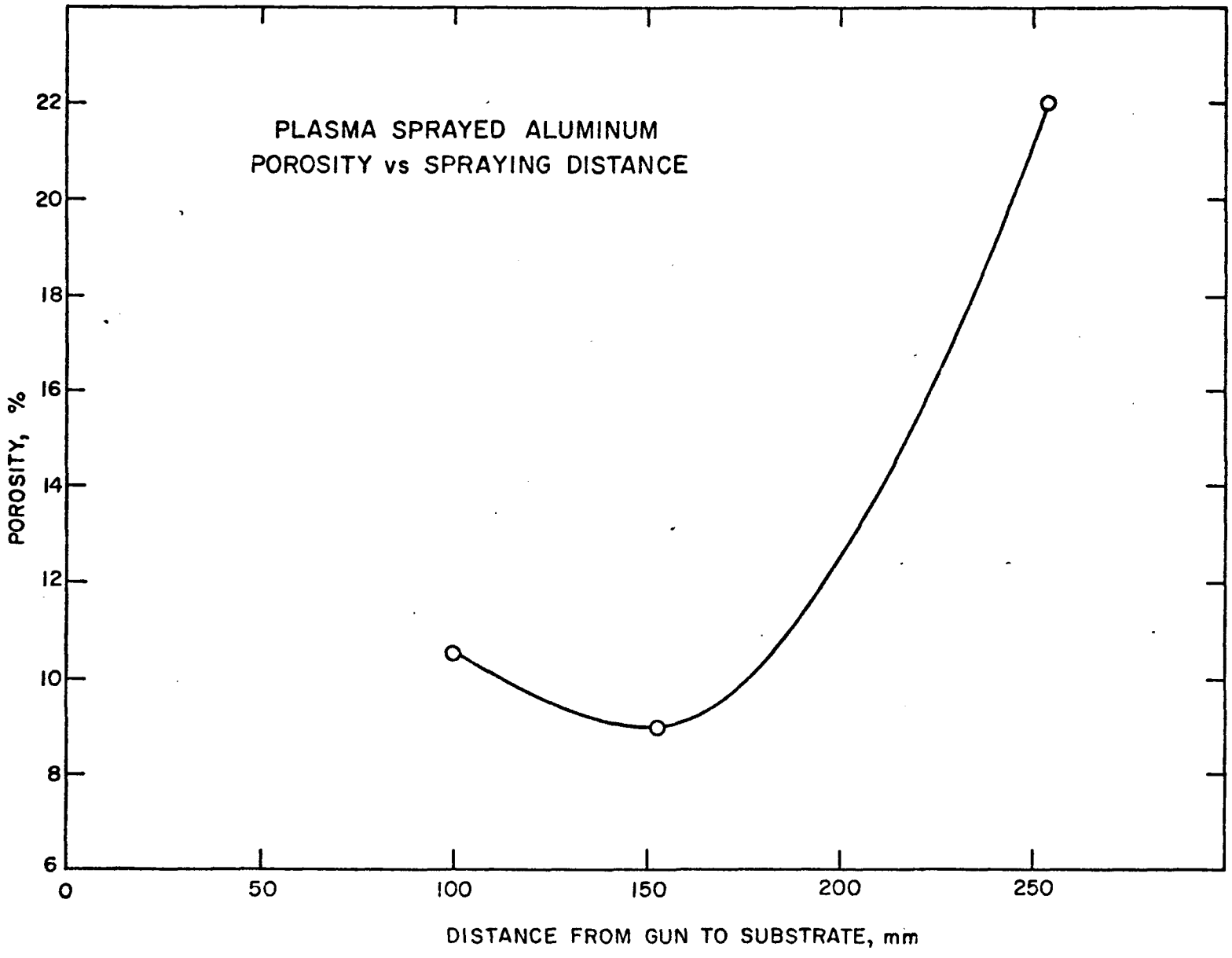

Fig. 6. Total pore volume versus sample/gun distance, ℓ.

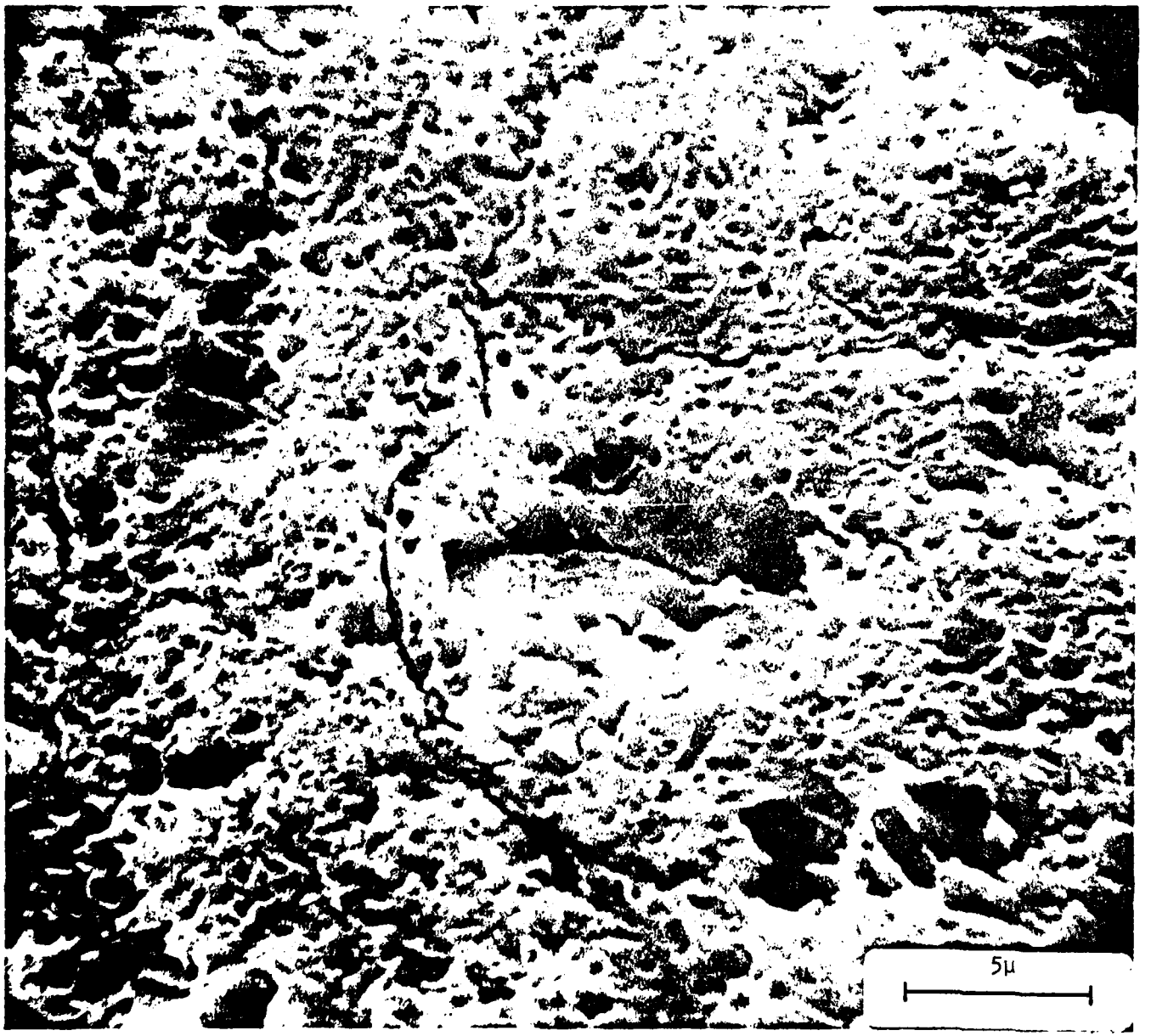

Fig. 7. Scanning electron micrograph of etched aluminum coating sprayed at a distance of 10 cm from the gun.

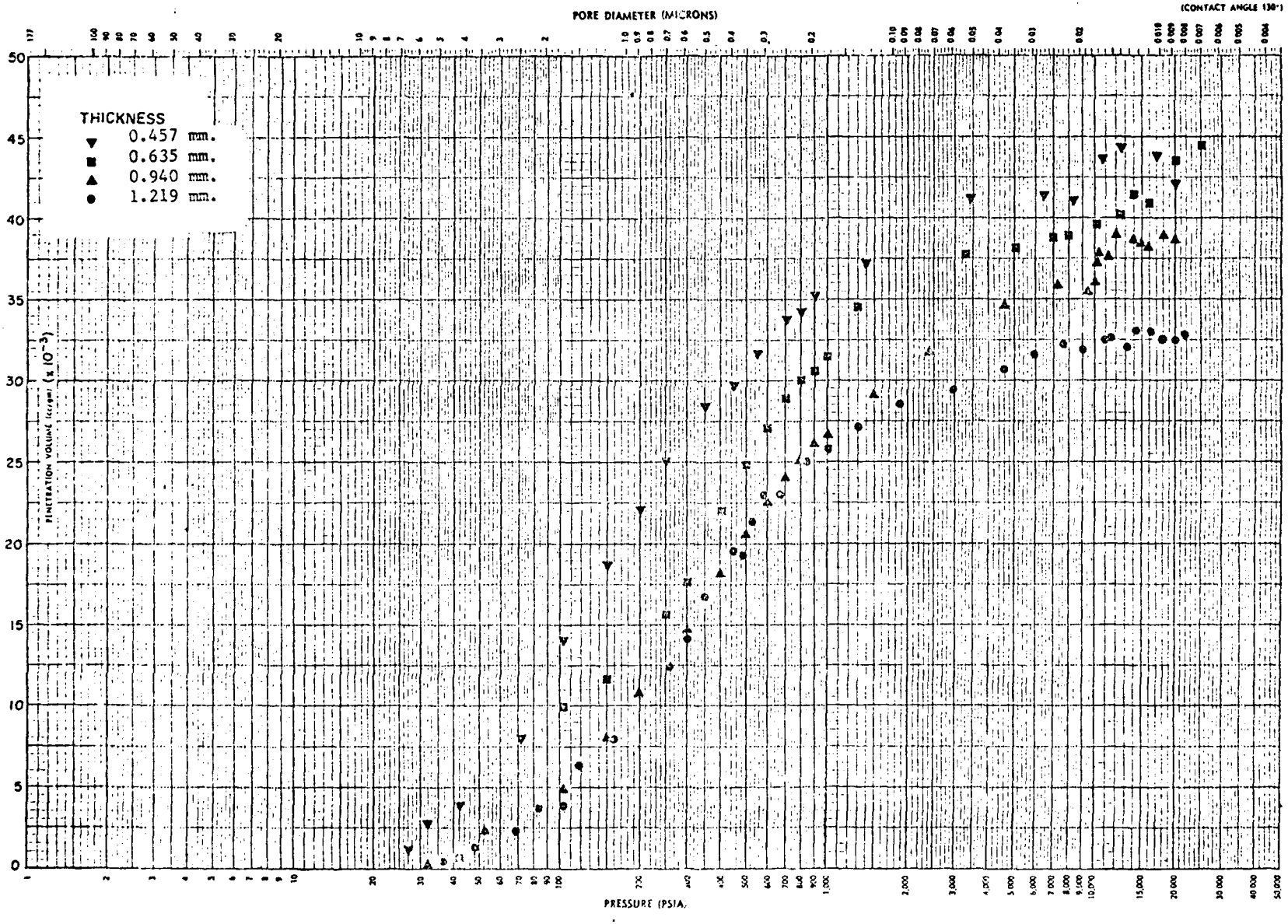

Fig. 8. Penetration of mercury into the coating versus applied pressure.

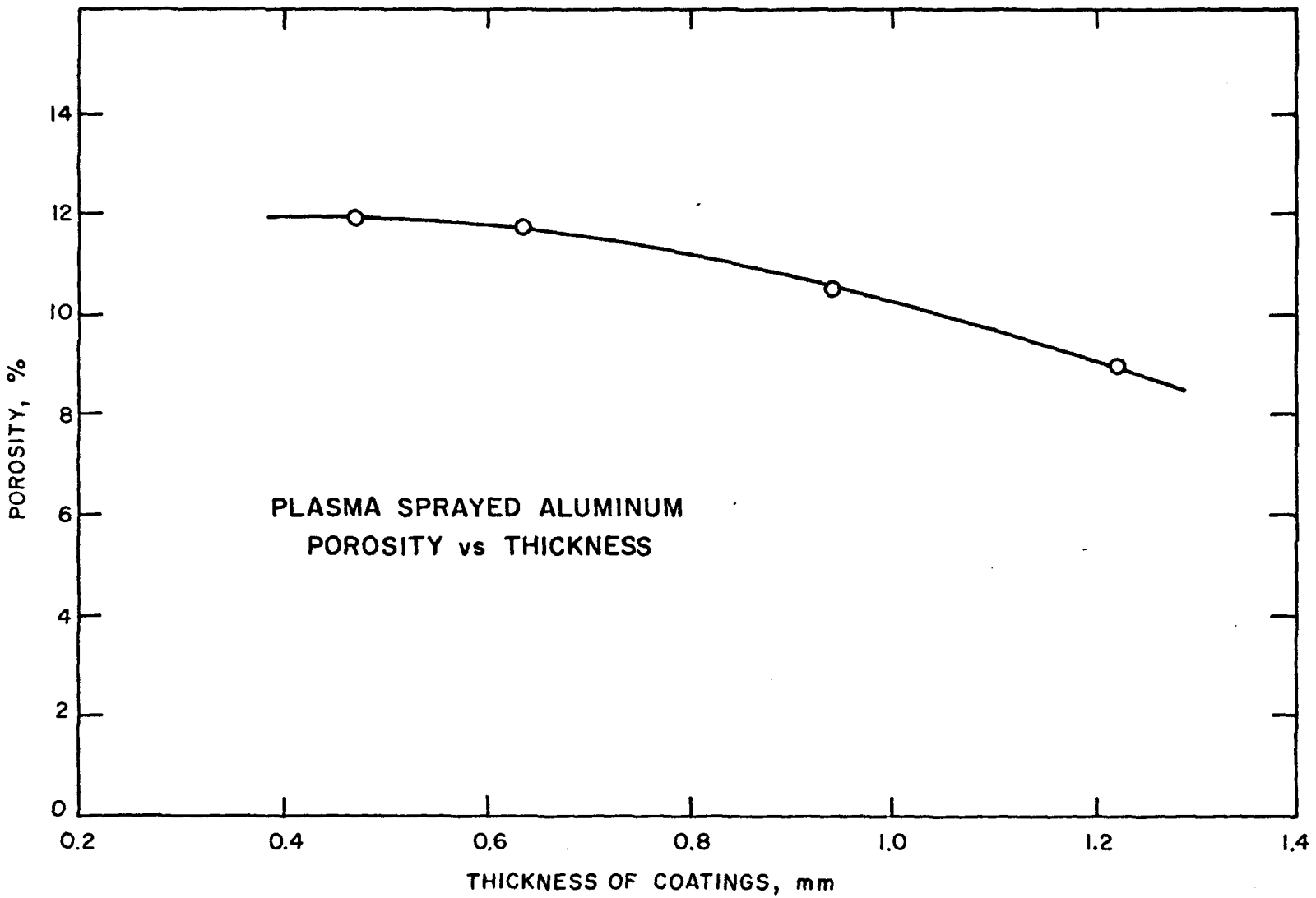

Fig. 9. Total pore volume versus thickness of coating.

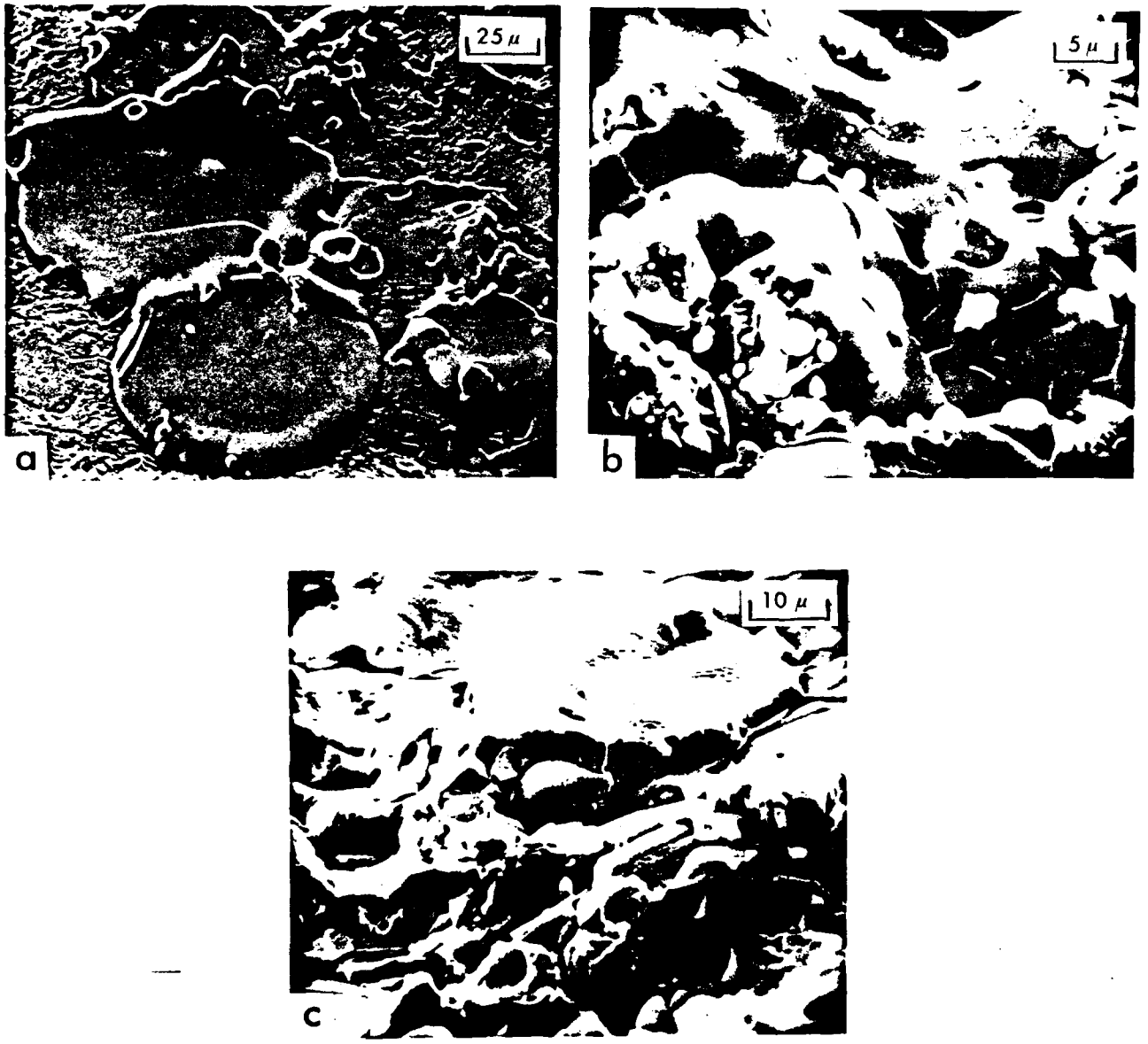

Fig. 10. Scanning electron micrographs of plasma-sprayed alumina on steel.
a) single droplets on etched steel surface;
b) typical coating surface;
c) typical cross-section of a coating, showing the lamellar structure.

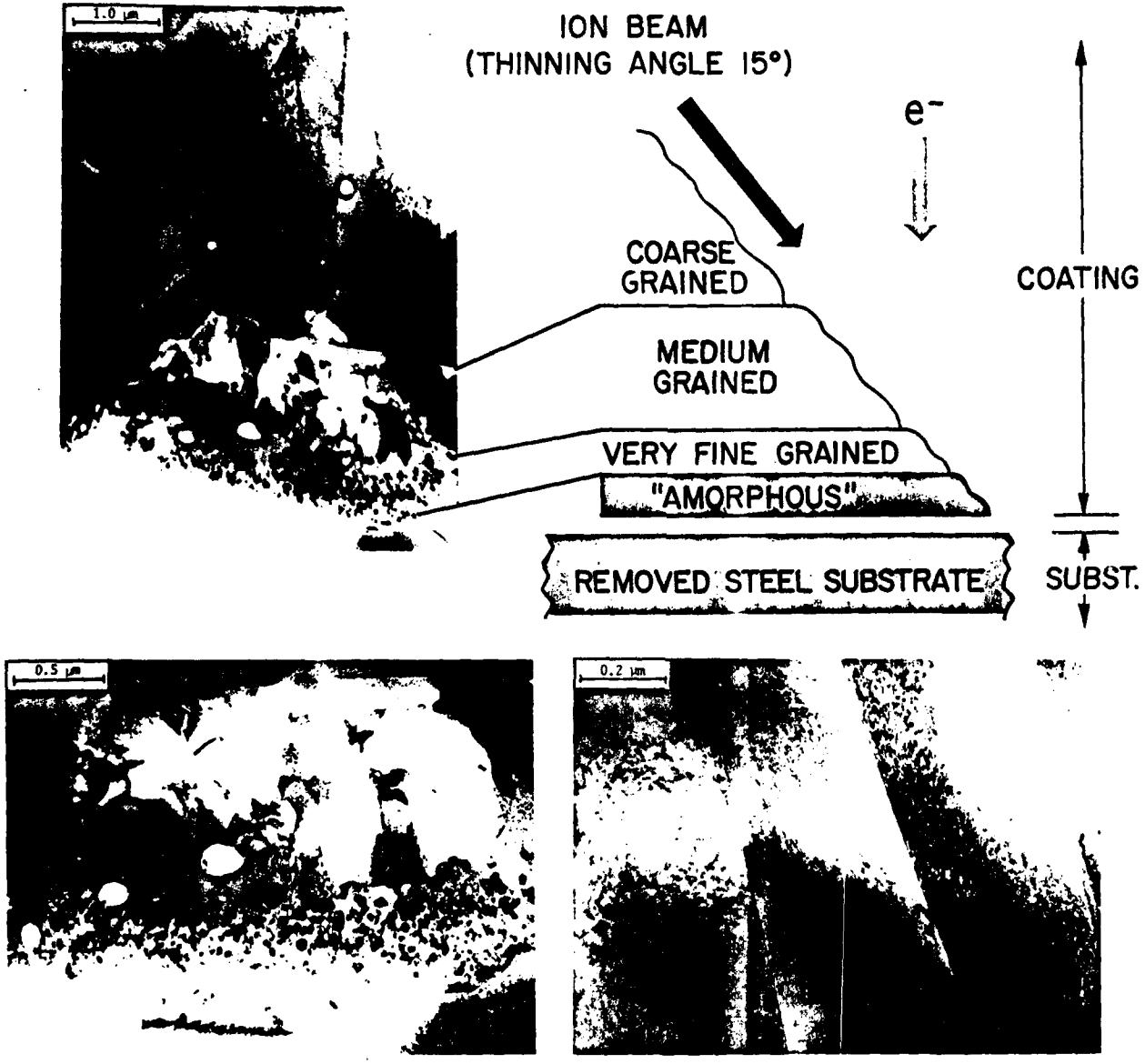

TYPICAL SECTION OF AN Al_2O_3 COATING

Fig. 11. TEM study of the interfacial region of plasma sprayed Al_2O_3. The lower micrographs show a magnified view of the first few layers (as seen above) and a typical grain structure at approximately 15 μm into the coating.

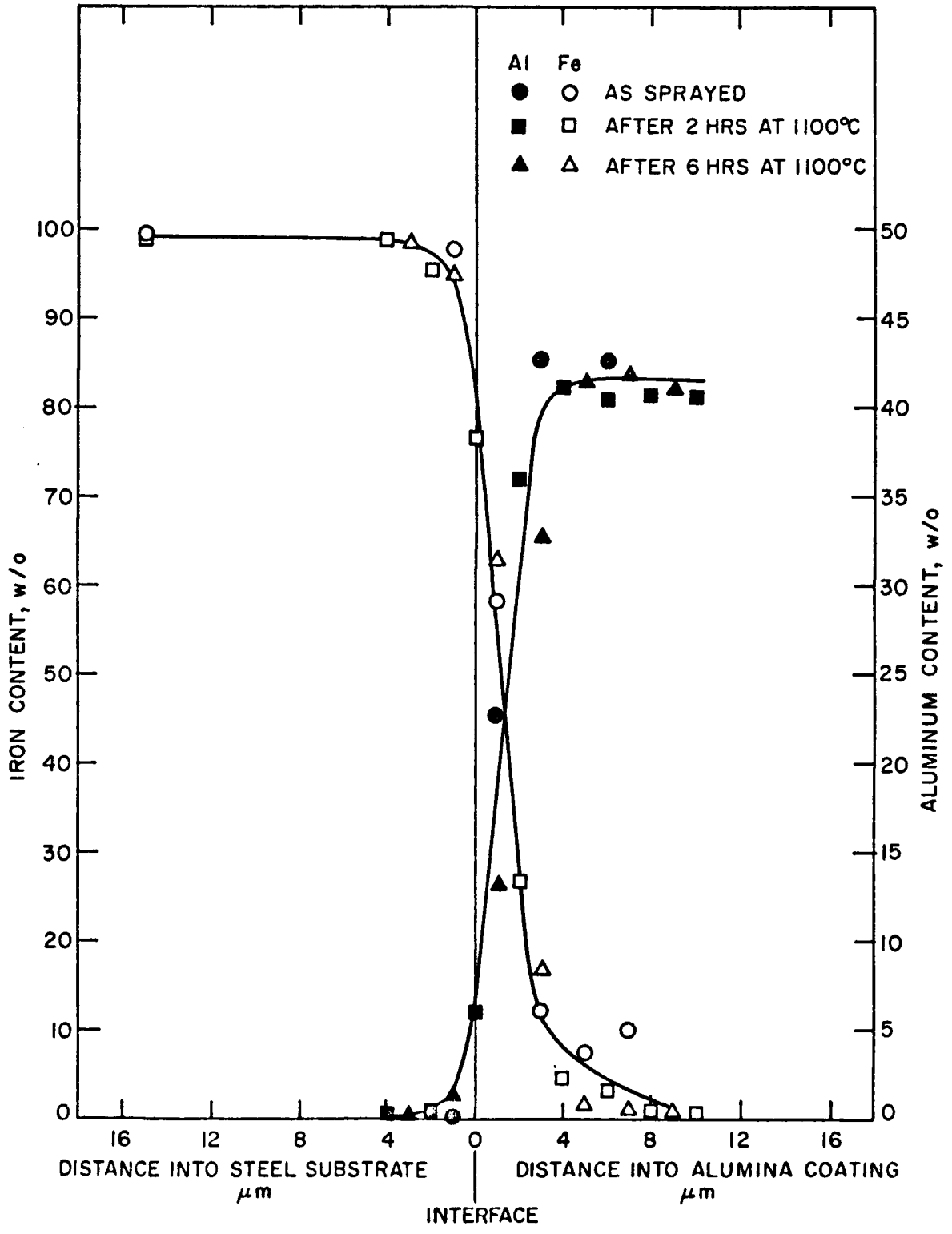

Fig. 12. Electron microprobe analysis of interdiffusion of iron and aluminum across the substrate/coating interface.

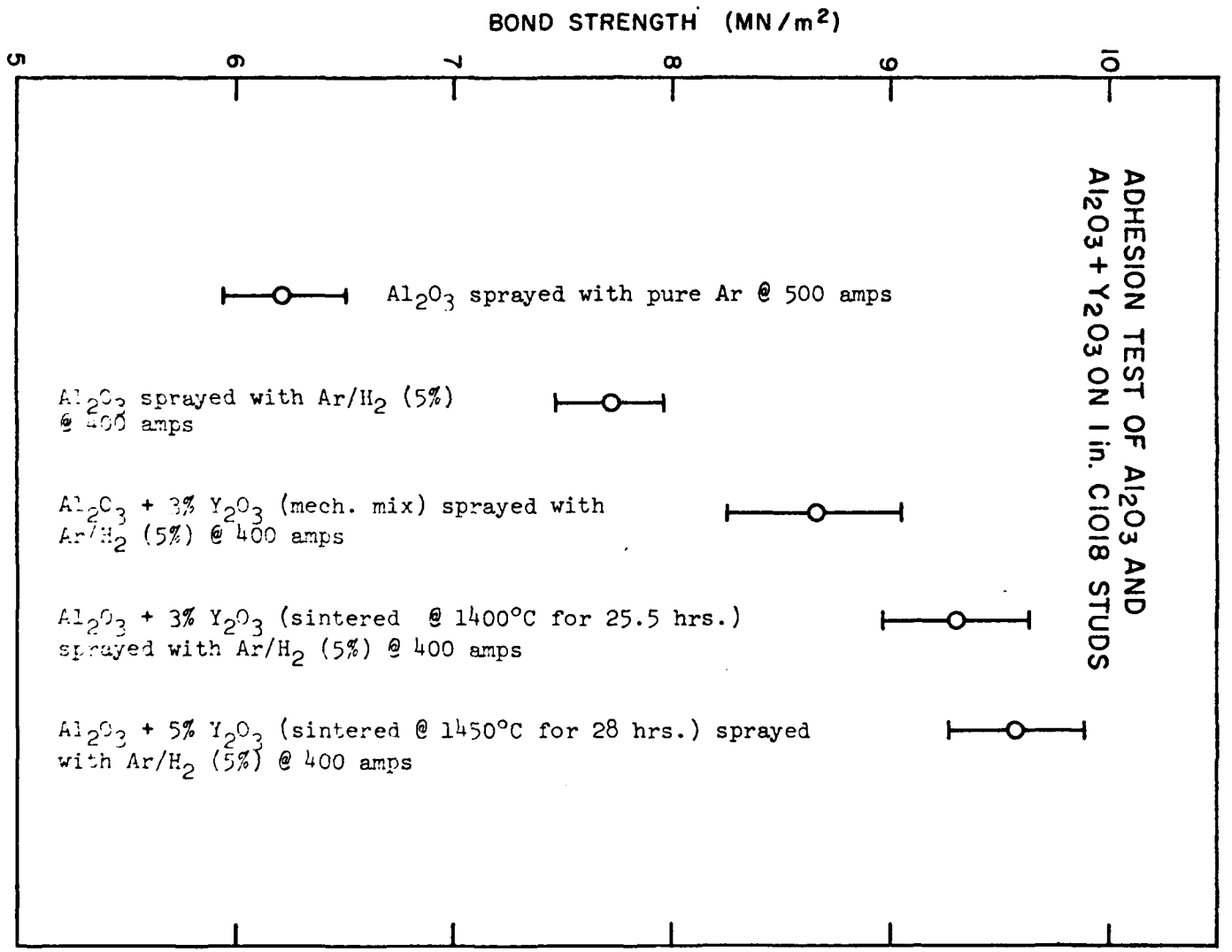

Fig. 13. The tensile adhesive strength of the Al_2O_3/steel substrate bond.

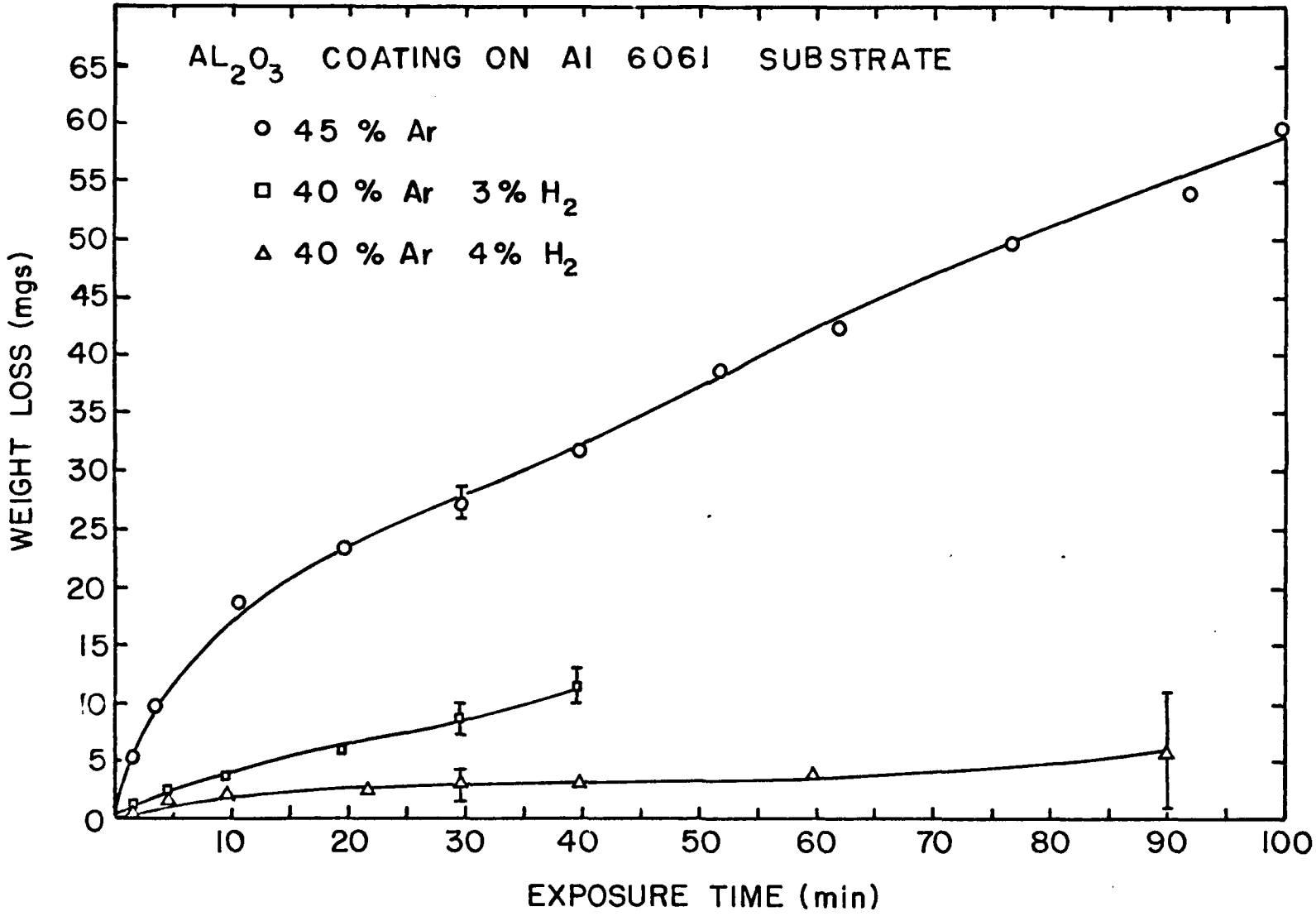

Fig. 14. The cavitation erosion rate of Al_2O_3 coated steels sprayed in different plasmas.

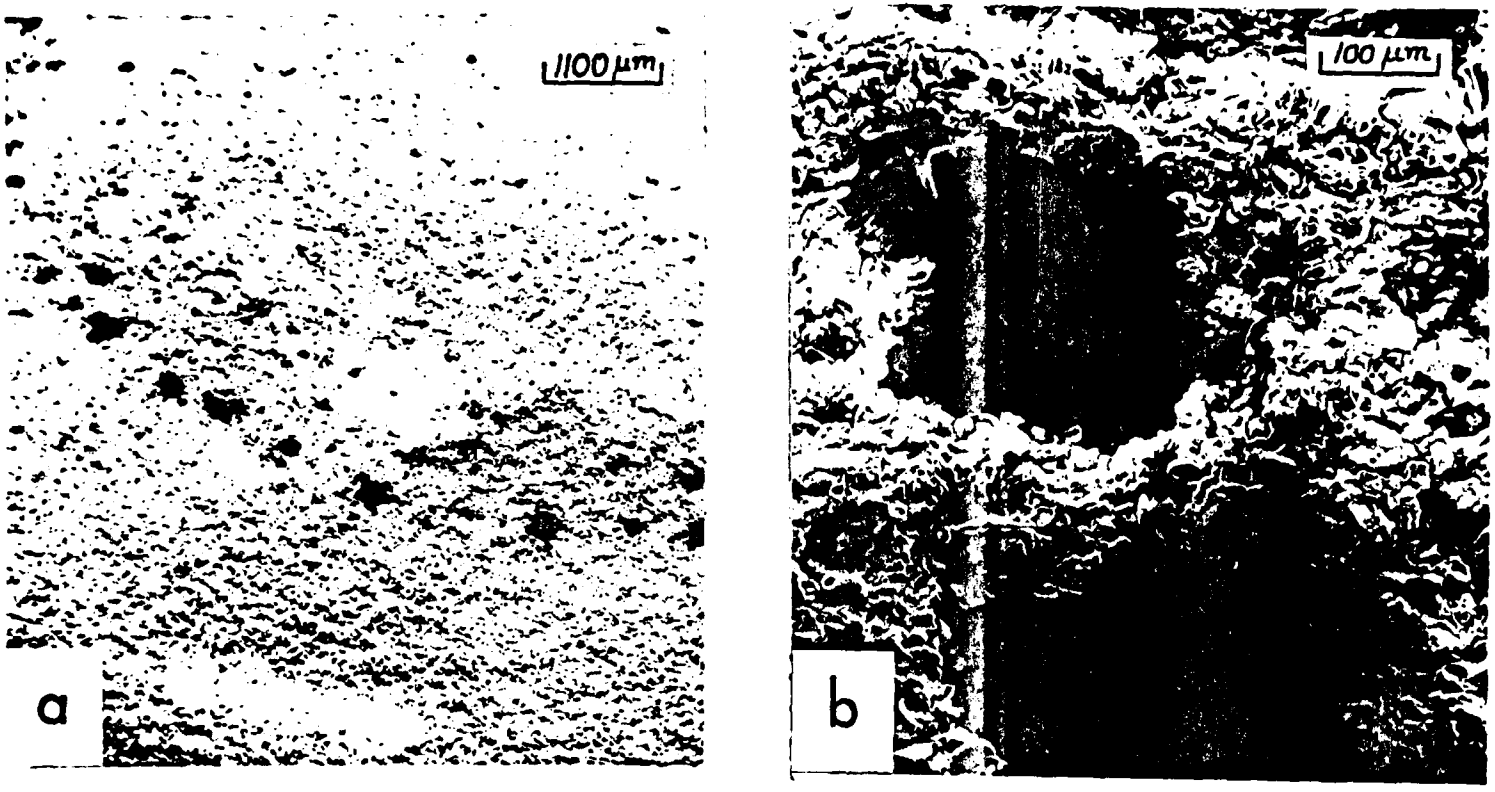

Fig. 15. Scanning electron micrograph of an Al_2O_3 coated steel after exposure to cavitation showing random pitting attack.

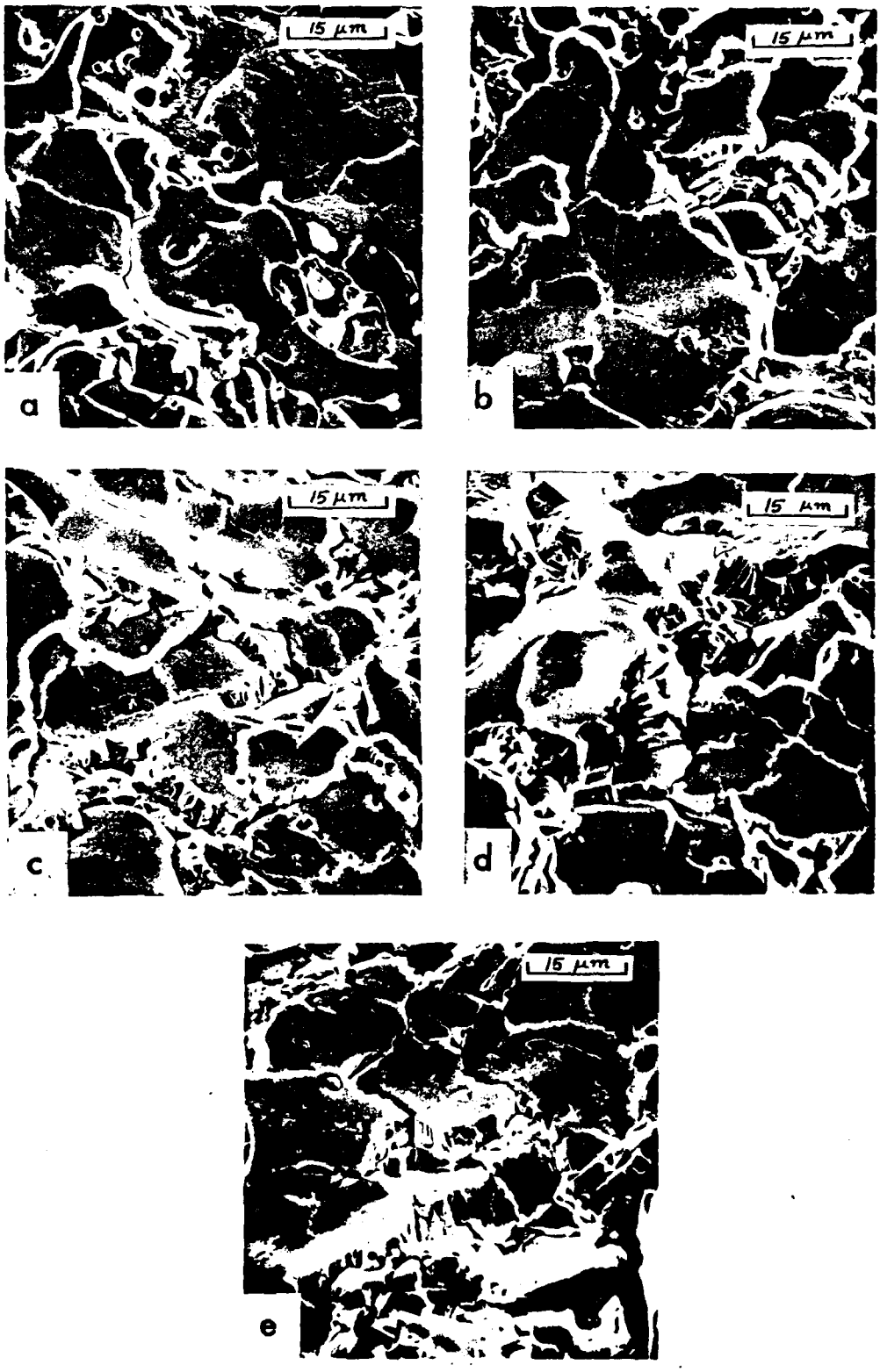

Fig. 16. Scanning electron micrographs of an Al_2O_3 coating exposed to cavitation for (a) 0, (b) 1 min. (c) 2 min. (d) 3 min. and (e) 4 min.